Int. J. Electrochem. Sci., 8 **(2013)** 5203 - 5212

International Journal of
ELECTROCHEMICAL
SCIENCE
www.electrochemsci.org

Synthesis and Characterization of Nano-Sized Nickel Aluminate Spinel Crystals

N. M. Deraz

Chemistry Department , College of Science, King Saud University, P.O. Box 2455, Riyadh 11451, Saudi Arabia
E-mail: nmderaz@yahoo.com

Received: 24 February 2013 / *Accepted:* 18 March 2013 / *Published:* 1 April 2013

X-ray diffraction (XRD) of nickel aluminate showed its structural properties such as crystallite size, lattice constant, unit cell volume and X-ray density. The nano-sized nickel aluminat ($NiAl_2O_4$) crystals were prepared in this study. The morphological properties and the surface concentration of elements involved in the spinel $NiAl_2O_4$ solid were studied by Scanning electron micrographs (SEM) and Energy dispersive X-ray (EDX) techniques. The results showed formation of single phase of nano-crystalline nickel aluminate with spinel structure. The nature of the as synthesized powders was spongy and fragile.

Keywords: XRD; SEM, EDX; $NiAl_2O_4$ nano-particles.

1. INTRODUCTION

Nano-crystalline spinel aluminates with the general formula MAl_2O_4 (M= Ni, Zn, Mn, Co and Mg…….etc) attract the research interest because of their versatile practical applications. Aluminates have high thermal stability, high mechanical resistance, hydrophobicity, and low surface acidity [1]. Nickel aluminates, one of the most important aluminate materials, have been studied for many applications, including magnetic materials, pigments, catalysts and refractory materials [2]. This aluminate is an inverse spinel in which eight units of $NiAl_2O_4$ go into a unit cell of the spinel structure. Half of the aluminum ions preferentially fill the tetrahedral sites (A-sites) and the other occupies the octahedral sites (B-sites). Thus, the compound can be represented by the formula $(Al^{3+})_A[Ni^{2+}Al^{3+}]_BO_4^{2-}$, where A and B represent tetrahedral and octahedral sites, respectively [3]. Its remarkable electrical and magnetic properties depend upon the nature of the ions, their charges and their distribution among tetrahedral (A) and octahedral (B) sites [3].

Composites consisted entirely of aluminum and aluminate spinel whiskers are of interest in aerospace and automobile industries. This could be attributed the combination of excellent properties of Al matrix and the whiskers, such as high specific strength and stiffness, good wear resistance, elevated temperature stability, and low cost of production [4–6]. Several researches have been carried out on aluminum matrix composites to improve their mechanical and thermal properties due to the promising applications in weight saving and energy conservation [7-9].

It is commonly known that nano-particles with controlled size and composition have fundamental and technological interest. The preparation method determines not only the products characteristics like size and shape, but also their physical properties. Aluminates are commonly prepared by the ceramic technique that involves high-temperature solid state reactions between the constituent oxides. The particles are large and of non-uniform size [10].

Several preparation methods have been studied to obtain crystalline nickel aluminate spinels with small particle size, such as sol gel synthesis, sono-chemical method, microwave heating and polymer solution route [2-14]. The essential requirements of obtaining well controlled uniformity and high-purity materials encouraged the development of wet chemical methods. One of the important methods to prepare aluminates is combustion route. The advantage of the solution combustion technique is the quasi-atomic dispersion of the component cations in liquid precursors, which facilitates synthesis of the crystallized powder with low particle size and high purity at low temperatures [3].

In the current study, we aim to prepare nickel aluminate via glycine-assisted combustion method. Another goal for this investigation is the study of the effect of glycine content on the structural and morphological properties of the as prepared nickel aluminate. The techniques employed were XRD, IR, EDX and SEM.

2. EXPERIMENTAL

2.1. Materials

Two Ni/Al mixed oxides were prepared by mixing calculated proportions of nickel and aluminum nitrates with two different amounts of glycine. The mixed precursors were concentrated in a porcelain crucible on a hot plate at 350 ^{o}C for 5 minutes. The crystal water was gradually vaporized during heating and when a crucible temperature was reached, a great deal of foams produced and spark appeared at one corner which spread through the mass, yielding a brown voluminous and fluffy product in the container. In our experiment, the ratios of the glycine: aluminum: nickel nitrates were (0 and 2): 1: 2 for S1 and S2 samples, respectively. In other words, the ratios of glycine to metal nitrates (G/N) were 0.00 and 0.67 for S1 and S2 samples. A general flowchart of the synthesis process is shown in Fig. 1. The chemicals employed in the present work were of analytical grade supplied by Fluke Company.

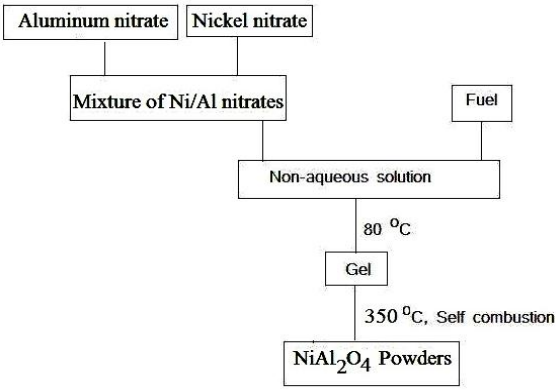

Figure 1. Process flowchart for fabricating the as prepared samples.

2.2. Techniques

An X-ray measurement of various mixed solids was carried out using a BRUKER D8 advance diffractometer (Germany). The patterns were run with Cu K_α radiation at 40 kV and 40 mA with scanning speed in 2θ of 2 ° min^{-1}.

The crystallite size of $NiAl_2O_4$ crystallites present in the investigated solids was based on X-ray diffraction line broadening and calculated by using Scherrer equation [15].

$$d = \frac{B\lambda}{\beta \cos\theta} \qquad (1)$$

where d is the average crystallite size of the phase under investigation, B is the Scherrer constant (0.89), λ is the wave length of X-ray beam used, β is the full-with half maximum (FWHM) of diffraction and θ is the Bragg's angle.

Scanning electron micrographs (SEM) were recorded on SEM-JEOL JAX-840A electron microanalyzer (Japan). The samples were dispersed in ethanol and then treated ultrasonically in order disperse individual particles over a gold grids.

Energy dispersive X-ray (EDX) analysis was carried out on Hitachi S-800 electron microscope with an attached kevex Delta system. The parameters were as follows: accelerating voltage 10, 15 and 20 kV, accumulation time 100s, window width 8 μm. The surface molar composition was determined by the Asa method, Zaf-correction, Gaussian approximation.

3. RESULTS

3.1. Structural analysis

The XRD diffractograms for S1and S2 samples are given in Fig. 2.

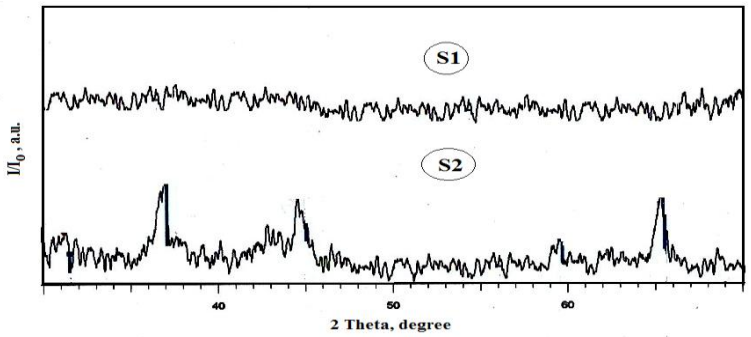

Figure 2. XRD patterns for the as prepared nickel aluminate ($NiAl_2O_4$) sample.

Preliminary Experiments showed that the increase in the amount of glycine to metal nitrate (G/N) led to absence of the spinel nickel aluminate. Examination of Fig. 1 revealed that: (i) The S1 sample consisted entirely of amorphous materials which may be nickel and aluminum oxides and/or Ni-Al- O compound. (ii) The S2 sample consisted of moderate crystalline $NiAl_2O_4$ particles as a single phase. Indeed, the XRD pattern contains ten sharp lines coincide with the standard data of the cubic spinel Ni aluminate phase (JCPDS card No. 10-0339). The peaks of the as prepared solid indexed to the crystal plane of spinel nickel aluminate (220), (311), (400), (511) and (440) respectively. The nickel aluminate crystallizes in spinel form with the space group *Fd*3*m*. This indicates that the presence of small amount of glycine (G/N = 0.67) led to stimulate the solid state between the reacting oxides (NiO and Al_2O_3) yielding $NiAl_2O_4$ crystallites. However, absence of nickel aluminate above the previous limit (G/N = 0.67) was observed.

The X-ray data enabled us to calculate the different structural parameters of cubic spinel nickel aluminate such as the crystallite size (d), lattice constant (a), unit cell volume (V), X-ray density (D_x), the distance between the reacting ions (L_A and L_B), ionic radii (r_A, r_B) and bond lengths (A–O and B–O) on tetrahedral (A) sites and octahedral (B) sites. The values of the previous structural parameters of nickel aluminate were tabulated in Tables 1 and 2.

Table 1. The values of d, a, V and D_x of the as prepared nickel aluminate.

Samples	d (nm)	a (nm)	V (nm^3)	D_x (g/cm^3)
S2	16	0.8083	0.5281	4.4422

Table 2. The values of L_A, L_B, A-O, B-O, r_A and r_B for the as prepared nickel aluminate sample.

Sample	L_A (nm)	L_B (nm)	A-O (nm)	B-O (nm)	r_A (nm)	r_B (nm)
S2	0.3499	0.2858	0.1820	0.1980	0.0469	0.0630

3.2. Formation of spinel $NiAl_2O_4$ compound

Spinel-type $NiAl_2O_4$ compound can be formed by the solid state reaction between both NiO and Al_2O_3 via the thermal diffusion for the cations of these oxides through the early layer of aluminate [16]. Deraz reported that the glycine assisted combustion method is useful for providing an alternative of low cost mass production of various spinel materials [17, 18]. The counter-diffusion of Ni^{2+} and Al^{3+} through a relatively rigid aluminates film led to the formation of $NiAl_2O_4$ particles. We speculate that the diffusing ions might be Ni^{2+} including Ni^{3+} on the basis of detecting Ni^{2+} in the interface. In addition, following reactions indicate that Al_2O_3 decomposes to $2Al^{3+}$ and oxygen gas at Al_2O_3-interface. Moreover, oxygen moves through the reacted area to be added to the NiO interface and form spinel by reacting with aluminum ions:

At Al_2O_3 interface:

$$3Al_2O_3 + 2Ni^{2+} \rightarrow 2NiAl_2O_4 + 2Al^{3+} + 0.5O_2 \qquad (2)$$

At NiO interface:

$$2Al^{3+} + 3NiO + 0.5O_2 \rightarrow NiAl_2O_4 + 2Ni^{2+} \qquad (3)$$

3.3. The morphology study

Figs. 3 and 4 show the SEM images for S1 and S2 samples, respectively. The SEM picture of the S1 specimen (Fig. 3) reveals agglomerated and larger (dense) particles with small light particles on the surface as shown in Fig. 3. In other words, it can be seen from this figure that the S1 samples consisted of two polygonal- shaped grains. The presence of these light particles is probably due to the influence of secondary phases. Indeed, the XRD measurements showed that the S1 sample contains amorphous materials which may be nickel and aluminum oxides and/or Ni-Al- O compound. But, addition of small amount of glycine to the Ni/Al precursors followed by heating in air at 350 ^oC for 5min. in a porcelain crucible on a hot plate led to formation of agglomerated, porous and flaky morphologies of $NiAl_2O_4$ particles. XRD measurements confirm synthesis of spinel nickel aluminate as a single phase. In other words, the glycine-assisted fabrication of nano-crystalline nickel aluminate system resulted in fluffy and foamy materials. Investigation of Fig. 4, related to the S2 sample, with high magnifications reveals that the as prepared $NiAl_2O_4$ system contains voids and pores. These voids and pores could be attributed to the release of large amounts of gases during combustion process due to decomposition of the glycine and Ni and Al nitrates.

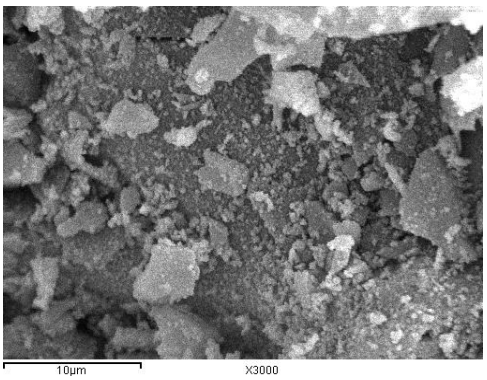

Figure 3. SEM images for the S1 sample.

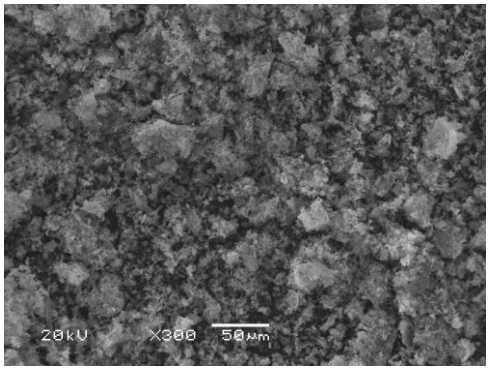

A

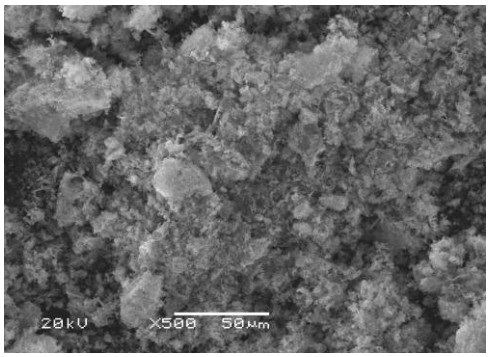

B

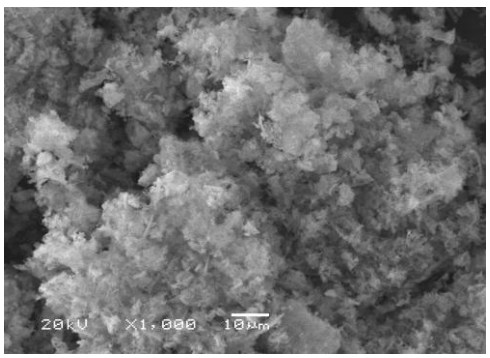

C

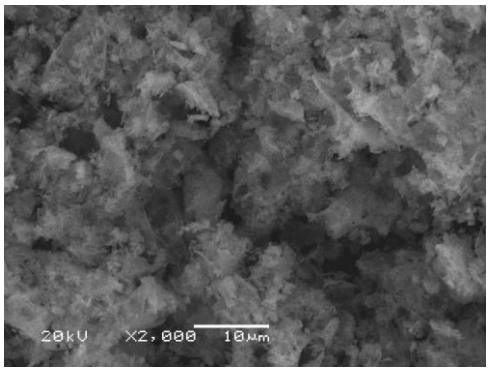

D

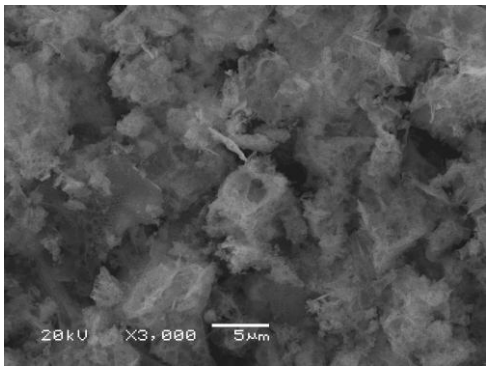

F

Figure 4. SEM images for the S2 sample with different magnifications.

3.4. Homogeneity of the as prepared samples

Different areas on surface of the S2 sample are considered by using energy dispersive X-ray (EDX) analysis at 20 keV as shown in Fig. 5.

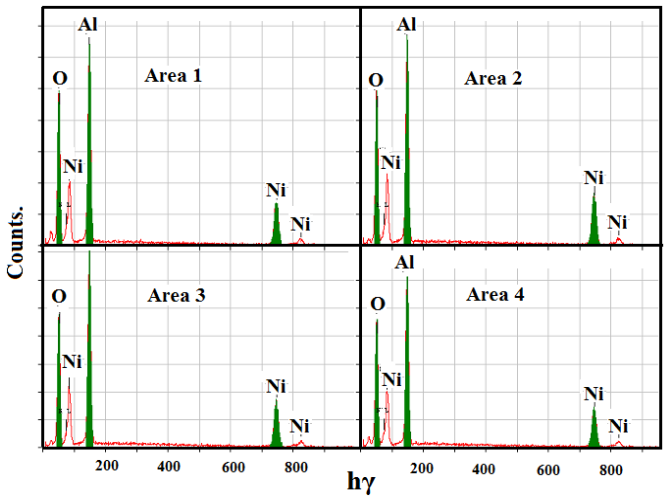

Figure 5. EDX pattern for the as prepared nickel aluminate sample at different areas.

Table 3 displays the relative atomic abundance of O, Ni and Al species present in the surface layers of The S2 sample. It can be seen from this table that the surface concentrations of O, Ni and Al species at 20 keV on different areas over the surface of specimens studied are much closed to each other. This indicates the homogeneous distribution of O, Ni and Al species in the samples studied. So, the combustion route resulted in production of homogeneously distributed materials. In other words, the combustion synthesis produces $NiAl_2O_4$ particles of a very uniform size.

Table 3. The atomic abundance of elements measured at 20 keV and different areas over the as prepared nickel aluminate sample.

Elements	Area 1	Area 2	Area 3	Area 4
O	33.47	32.74	32.97	33.31
Ni	41.67	43.91	43.19	42.15
Al	24.86	23.35	23.84	24.54

3.6. The elements gradient

Figure 6 showed the concentrations of Ni, Al and oxygen species from the uppermost surface to the bulk layers for the S2 sample by using the EDX investigation at 5, 10, 15 and 20 keV.

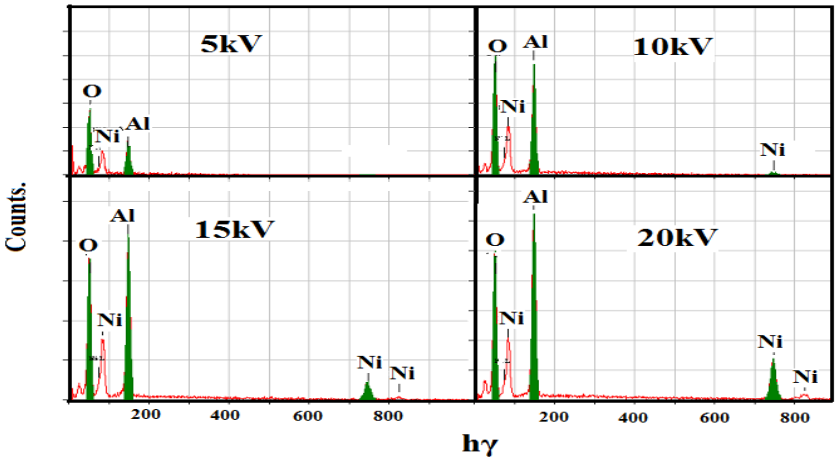

Figure 6. EDX pattern for the as prepared nickel aluminate sample at different applied voltages.

The concentrations of Ni, Al and oxygen species at 5, 10, 15 and 20 keV for the S2 sample are summarized in Table 4. Inspection of this table revealed that: (i) the surface concentrations of Al and oxygen species for the S2 sample decrease as the applied voltage increases from 5 to 20 keV. This indicates that the uppermost surface layer of the S2 sample is O- and Al-rich layer. (ii) The absence of the Ni species at uppermost surface layer of this sample. The increase in the applied voltage above the previous limit (5 keV) showed that the surface concentrations of Ni species increase from the

uppermost surface layer to the bulk of the as prepared materials. These findings suggest a possible redistribution for the essential elements involved in the as synthesized nickel aluminate with subsequent unique properties of this aluminate.

Table 4. The atomic abundance of elements measured at different voltages over the same area for the as prepared nickel aluminate sample.

Elements	Atomic abundance (%)			
	5 keV	10 keV	15 keV	20 keV
O	47.07	41.57	35.94	33.50
Ni	00.00	16.87	34.10	41.58
Al	52.93	41.57	29.96	24.93

5. CONCLUSIONS

Glycine-assisted combustion route resulted in formation of spinel $NiAl_2O_4$ nano- particles as a single phase. The powder XRD data obtained on $NiAl_2O_4$ powder are in good agreement with the standard reported data. the values crystallite size, lattice constant, unit cell volume and X-ray density of $NiAl_2O_4$ are 16nm, 0.8083 nm, 0.5281 nm^3 and 4.442 g/cm^3 . The SEM pictures show the presence of fluffy morphology found in the powder. The obtained samples have a homogenously distributed species in the whole mass prepared.

ACKNOWLEDGEMENT
This project was supported by King Saud University, Deanship of Scientific Research, College of Science Research Centre.

References

1. M. Zawadzki, J. Wrzyszcz, *Mater. Res. Bull.*, 35 (2000) 109.
2. J.W. Kim, P.W. Shin, M.J. Lee, S.J. Lee, *J. Ceramic Processing and Research*, 7(2006)117.
3. K. Christine Stella, A. Samson Nesaraj, *Iranian Journal of Materials Science & Engineering, 7(2010)*36.
4. S. Sheibani, M. F. Najafabadi, *Mater. Des.*, 28(2007)2373.
5. Fei WD, Hu M, Yao CK. *Mater. Chem. Phys.*, 77(2003)882.
6. Y.C. Feng, L. Geng, P. Q. Zheng, Z. Z. Zheng, G. S. Wang, *Mater. Des.*, 29(2008)2023.
7. W. A. Uju, I. N. A. Oguocha, *Mater. Des.*, 33(2012)503.
8. Y . Wang, W. M. Rainforth, H. Jones, M. Lieblich, *Wear*, 251(2001)1421.
9. Zhou Yang, Yu Zhenyang, Zhao Naiqin, Shi Chunsheng, Liu Enzuo, Du Xiwen, He Chunnian, *Mater. Des.*, 46 (2013) 724.

10. A. Yamakawa, , M. Hashiba, Y. Nurishi, *J. Mater. Sci.*, 24(1989)1491.
11. C.O. Arean, M. P. Mentruit, A.J. Lopez, Parra, J.B., *Coll. Surf. A*, 180(2001)253.
12. F. Meyer, R. Hempelmann, S. Mathur, M. Veith, *J. Mater. Chem., 9(*1999)1755.
13. P. Jeevanandam, Yu Koltypin, A. Gedaanken, *Mater. Sci. Eng. B*, 90(2002)125.
14. M. Mohammadpour Amini, L. Torkian, *Matter. Lett.*, 57(2002)639.
15. B.D. Cullity, Elements of X-ray Diffraction, Addison-Wesly Publishing Co. Inc. 1976 (Chapter 14).
16. Yamakawa, A., Hashiba, M. and Nurishi. Y., *J Mater. Sci.*, 1989, 24, 1491.
17. N. M. Deraz, *Ceramics Internationa,l* 38 (2012) 511.
18. N. M. Deraz, *Int. J. Electrochem. Sci.,* 7(2012) 4596.